



University of HUDDERSFIELD

University of Huddersfield Repository

Wang, Jian, Leach, R.K. and Jiang, Xiang

Review of the mathematical foundations of data fusion techniques in surface metrology

Original Citation

Wang, Jian, Leach, R.K. and Jiang, Xiang (2015) Review of the mathematical foundations of data fusion techniques in surface metrology. *Surface Topography: Metrology and Properties*, 3 (2). ISSN 2051-672X

This version is available at <http://eprints.hud.ac.uk/id/eprint/24794/>

The University Repository is a digital collection of the research output of the University, available on Open Access. Copyright and Moral Rights for the items on this site are retained by the individual author and/or other copyright owners. Users may access full items free of charge; copies of full text items generally can be reproduced, displayed or performed and given to third parties in any format or medium for personal research or study, educational or not-for-profit purposes without prior permission or charge, provided:

- The authors, title and full bibliographic details is credited in any copy;
- A hyperlink and/or URL is included for the original metadata page; and
- The content is not changed in any way.

For more information, including our policy and submission procedure, please contact the Repository Team at: E.mailbox@hud.ac.uk.

<http://eprints.hud.ac.uk/>

Review of the mathematical foundations of data fusion techniques in surface metrology

Jian Wang^a, Richard K Leach^{b,*}, X Jiang^a,

^aEPSRC Centre for Innovative Manufacturing in Advanced Metrology, University of Huddersfield, Huddersfield HD1 3DH, UK

^bDepartment of Mechanical, Materials and Manufacturing Engineering, University of Nottingham, Nottingham NG7 2RD, UK

*Correspondence author.

Email address: richard.leach@nottingham.ac.uk

Abstract

The recent proliferation of engineered surfaces, including freeform and structured surfaces, is challenging current metrology techniques. Measurement using multiple sensors has been proposed to achieve enhanced benefits, mainly in terms of spatial frequency bandwidth, which a single sensor cannot provide. When using data from different sensors, a process of data fusion is required and there is much active research in this area. In this paper, current data fusion methods and applications are reviewed, with a focus on the mathematical foundations of the subject. Common research questions in the fusion of surface metrology data are raised and potential fusion algorithms are discussed.

Keywords: surface metrology, data fusion, multiple sensors

1. Introduction

Multi-sensor data fusion is currently one of the considered solutions for the measurement of freeform and high dynamic range structured surfaces. A comprehensive review of the application of data fusion techniques in dimensional metrology has been published elsewhere [1], but excluded some important research work on the development of fusion algorithms for surface metrology. The review presented here aims to be complimentary to the previous published work.

1.1. Background

Currently, structured and freeform surfaces, which are engineered for a variety of functional uses in different disciplines, are under development for many applications [2-4]. Typical examples include diverse freeform structures [5,6], and structured surfaces such as friction-resistant feature arrays, broad spectrum absorption surfaces and self-cleaning surfaces, which are engineered with repetitive structures on the micro-/nano-scale [7]. Such surfaces need full 3D characterisation (often referred to as “holistic measurement” [1]) with relatively large sensing areas and high resolutions, which challenges current measurement techniques. For example, the 3D freeform sculpture surfaces presented in [8] cannot be fully measured in any acceptable amount of time using any of the instruments covered in current ISO specification standards [9].

1.2. The proposal and the objectives

All types of surface measuring instrument have advantages and disadvantages [1]. For example, tactile coordinate measuring machines (CMMs) are regarded as the most accurate instrument for macro-scale 3D measurement; however, they are expensive and it is time-consuming to obtain high-resolution 3D scanning data even for a relatively simple object. Instruments designed to measure surface texture, for example, coherence scanning interferometers (CSIs), have high axial resolution; however, they are only suitable for the measurement of topography on the micro- to nano-scales. A full measurement of a structured surface using CSI can require thousands of individual measurements of different areas. X-ray computed tomography is capable of measuring complex 3D structures; however, the measurement accuracy is normally low [10].

The combined use of different sensors can maximise the advantages of individual tools but avoid some of the disadvantages. Simple integration of multiple sensors in one system without actual combination of data is an initial step towards this objective. For example, the Leica DCM8 surface metrology system integrates interferometry and focus variation microscopy to increase the versatility of the system [11]. WITec GmbH

integrates confocal Raman microscopy, atomic force microscopy and scanning near-field optical microscopy into a versatile system which is capable of increasing the speed of the measurement of large area samples [12].

Data fusion, which integrates multiple datasets from different sources for a unified output, is a further step to the sensor integration techniques described above. The aim of data fusion is to combine the advantages of the data from different sensors so that the fused data has improved quality or usability over that from any individual datasets. The benefits of data fusion usually include improved measurement reliability and information completeness (for example, with larger measuring range coverage or higher sample resolution) [13]. In surface metrology, the potential benefits of data fusion specifically include any of the following:

1. increased spatial coverage or measuring range;
2. increased sample density or resolution;
3. improved reliability or fidelity, *i.e.* improved accuracy with improved robustness to sensory and algorithmic uncertainty;
4. reduced measuring duration; and
5. reduced data size.

1.3. Definitions

Data fusion has been used for data manipulation since the 1960s [14]. Data fusion received wide attention from the US defence sector, where the definition of data fusion and related terminologies were first standardised [15] in 1991 by the Joint Directors of Laboratories of the US Department of Defence. In this “Data Fusion Lexicon” [15], data fusion is defined as a “process dealing with the association, correlation and combination of data and information from single or multiple sources to achieve some improved estimation or assessments”.

The definition of data fusion in different disciplines varies [16]. In surface or dimensional metrology, the development of data fusion is still at an early stage. The data obtained in surface metrology is a type of spatial data [17]. Fusion of spatial data has specific characteristics, in contrast to other types of data, such as time-series, colour and acoustic data. For example, different surface measurement data need to be converted to a common format for combination, such as images with the same resolution, point clouds, statistical or functional models. Therefore, data fusion in surface or dimensional metrology is defined as [1]:

The process of combining data from several information sources (sensors) into a common representational format in order that the metrological evaluation can benefit from all available sensor information and data.

1.4. Fusion levels

The spatial data used in surface metrology can be fused at different levels, including the signal level, feature level and decision level [1,18]. The signal level is the elementary fusion level in which the input data are fused in their original form. The feature level is an intermediate fusion level in which signal descriptors are fused. The decision level is the highest fusion level in which the decisions (for example, classification results) from individual measurements are fused. Fusion on higher levels can be more efficient, but may be more restrained for a specialised purpose. In surface metrology, fusion at the signal level is usually the most common situation. For example, fusion of AFM and CSI range images is carried out at a pixel (signal) level [19]. However, advanced fusion algorithms or solutions for surface metrology data could be developed at other fusion levels.

1.5. Classifications

The sensor configuration determines the relationship between the individual datasets. Different relationships determine the manner in which fusion is applied [20]. The following four fusion classifications are applied in current surface measurement applications.

- 1) Fusion across sensors

The data comes effectively from multiple sensors or repeated measurements (with a single sensor) measuring the same attribute (for example, surface topography) of an object. Often redundancy in the data will be used to reduce error. Data from different sources in this class of fusion are homogeneous, for example, the datasets have the same resolution, uncertainty and measuring ranges.

2) Fusion across attributes

The input data corresponds to different attributes of the same object and have to be fused according to a relational model, taking into account the physical nature of the attributes, to gain as complete a picture as possible of the object from its component attributes. For example, given different attributes of a surface, such as surface roughness, hardness and heat transfer coefficients, a multi-variant analysis [21] of the information may find relational models between the attributes which can guide the control of the attributes in the processes of design and manufacture.

3) Fusion across domains

Data acquired at different scales, ranges or domains are fused to give a complete picture of the same object. Measurement results in different domains may include the measured range images of an object at different measuring scales, ranges, viewpoints and exposure conditions. Sometimes, the information in the domain of light intensity or colour is fused with the spatial information of an object. Fusion across domains is the most common case of data fusion used when measuring surface geometry, including the well-known “sub-aperture stitching” for large area surfaces [22]. The source data used for fusion can be homogeneous (for example, same-resolution range images captured at different positions), or inhomogeneous (for example, data from a CSI and a tactile system, computed tomography, or even non-geometry measurement tools).

4) Fusion across time

In this class of fusion, the data obtained from the same single or multiple sensors at different times are fused using a Kalman filter [23]. For example, a sensor detects a series of observations of the same surface at different times, and then a recursive fusion of the observation results can give an averaged estimation of the “real” surface geometry.

Among these classes of fusion, fusion across domains is the most general situation in surface metrology but the algorithms for this class of fusion have not been well developed.

In the following sections, the existing applications of data fusion in surface metrology are briefly reviewed. Then the common issues in general fusion activities for surface metrology are discussed. Finally, the fusion algorithms themselves are reviewed.

2. Existing data (sensor) fusion applications

2.1. Image fusion for dimensional information

Image fusion has been used for many years in signal processing and is a typical case of data fusion. In surface metrology, fusion of grey-scale or full colour images, such as fringe images, is used with the majority of instruments for measuring surface topography. For example, most topography instruments based on optical methods [24] use a single sensor to successively capture individual images and combine them to present the dimensional information for an object. Other applications of image fusion for dimensional metrology include shape from shading, photogrammetry, fringe (structured light) projection systems and deflectometry [1]. Due to the difference in sensing principles and sensor configurations, the fusion algorithms applied to each measuring systems differ. It is, therefore, not possible to describe the diverse algorithms in a common framework. In other words, research on image fusion algorithms for different sensing approaches cannot be inductively used to develop new fusion algorithms.

This section gives three typical examples of image fusion to give dimensional information in surface metrology. More examples of image fusion for surface and dimensional metrology can be found elsewhere [1].

1) Focus variation systems

Focus variation systems [24-26] were developed to achieve topography measurement of the top surfaces of an object by searching for the best focus position at each point on a sample. As shown in Figure 1, a series of images related to different depths are firstly obtained. Focus searching is then performed to find the focus depth for each pixel position and then a 3D rendering of the surface geometry is calculated. The core algorithm in this image fusion case searches for the focus position at each pixel position in the image stack, which has the highest contrast ratio when compared to its neighbouring pixels.

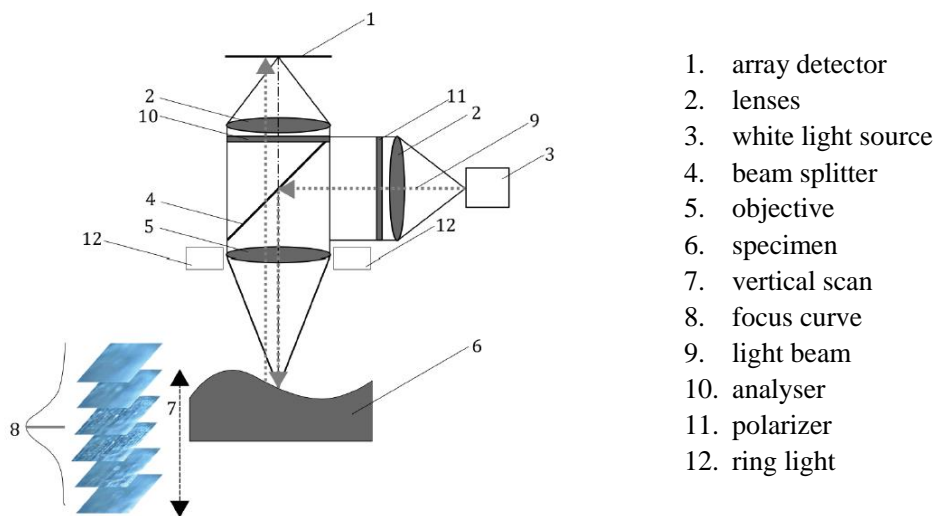


Figure 1. Schematic diagram of a typical focus variation system [26].

2) Coherence scanning interferometry

Another application of image fusion can be found in CSI systems [24,27,28]. Figure 2a presents how the fringe images differ at different scanning positions on the z -axis for a typical CSI system. At a specific pixel position in the image, the irradiance received by the camera varies as an envelope wave depending on the scanning positions on the z -axis (see Figure 2b). Usually, the z -scanning position which corresponds to the strongest irradiance can be inferred as the surface height or depth. The task of image fusion for CSI is to find the peak or centre position of the irradiance signal received at each pixel position, given a stack of fringe images acquired at different z positions. Different peak/centre searching methods (fusion algorithms) have been developed (for example, [29,30]) for the CSI image fusion process.

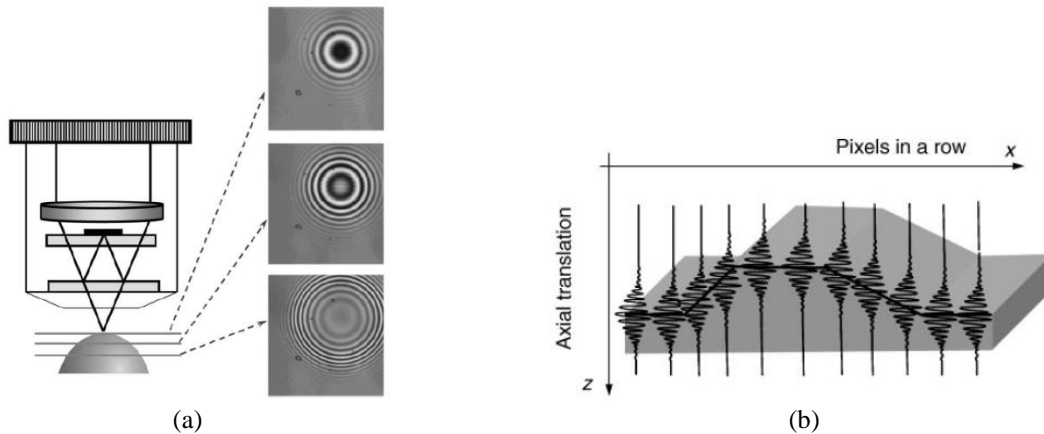


Figure 2. The CSI working principle. (a) Fringe images observed on a curved surface. (b) Irradiance signal observed for each pixel position against the scanning positions on the z-axis [28].

3) Computed tomography

X-ray computed tomography (XCT) is increasingly being applied for non-destructive 3D surface measurement in engineering with an uncertainty down to micrometres [31,32]. An XCT system radiates X-rays in a cone or parallel form through the object and detects the attenuated projection images (radiographs). By exposing the object from different directions, a stack of 2D images are obtained which are then fused to reconstruct [33] the volumetric information about the object (see Figure 3). The fusion algorithms for XCT are often based on Radon backprojection, but see elsewhere for a short review of different reconstruction algorithms [32].

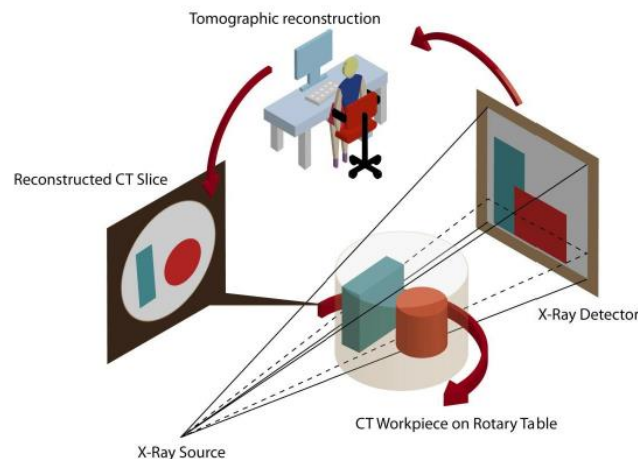


Figure 3. The working mechanism of a XCT system (courtesy of NPL [32]).

2.2. Computed visual fusion

Computed visual fusion is a process of applying visual sensors (such as video cameras) and geometrical measurement sensors to achieve automated measurement with the assistance of computers. Visual fusion provides the potential for automated manufacture and measurement in engineering. For example, a vision system based on video cameras can provide a preview or approximate contour knowledge about an object and then intelligent sampling using CMMs or other sensors for features of interest can be conducted in an efficient manner. Much research has been conducted for automated CMM metrology [34-37]. AFM systems have also recently been integrated with vision systems to achieve automatic, fast and large area measurements [38,39].

It should be noted that the data from vision systems and geometrical measurement systems are used in a temporal sequence. The final output of such fusion systems is generated solely from the geometrical measurement sensors. In other words, it is an elementary sensor fusion rather than data fusion that occurs in visual fusion cases.

2.3. Spatial data fusion

1) Repeated measurements

Using repeated measurements is well-known as a statistical method to reduce the uncertainty of a measurement. In surface or dimensional metrology, repeated measurements are widely used. For example, in a CSI, a sequence of measurement data from the same sensor can be obtained and averaged using the arithmetic mean (or weighted mean). If each individual data set has random noise or defects induced by uncertain environmental conditions, for example temperature, air flow, illumination, vibration, and electromagnetic disturbances, the mean output can be provided with higher reliability (lower uncertainty) [40]. Figure 4 shows the effect of a simple mean-based fusion for two noisy datasets acquired from a step signal.

In some fusion situations, the measuring environment can be manually altered to obtain different results which can compensate each other. For example, by altering the lighting conditions, a sphere surface can have different measurement results under the same CSI system [41]. Figure 5 presents the resultant measurement data under different light settings. The lower light level result has valid data acquired at the flat region, *i.e.* the sphere top and the base, but has missing data at the inclined regions. The higher light level result presents complementary data. An appropriate combination of the datasets can produce a result with a larger number of valid sample points, *i.e.* higher information completeness. Figure 5c presents such a fused result by combining the two image datasets in a point-wise manner using the maximum sample value.

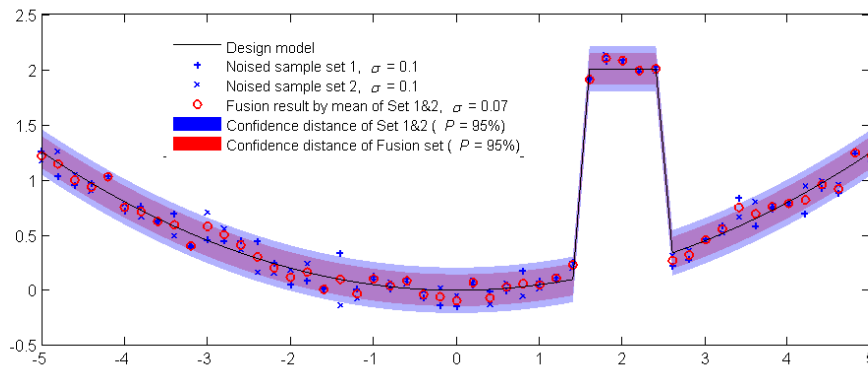
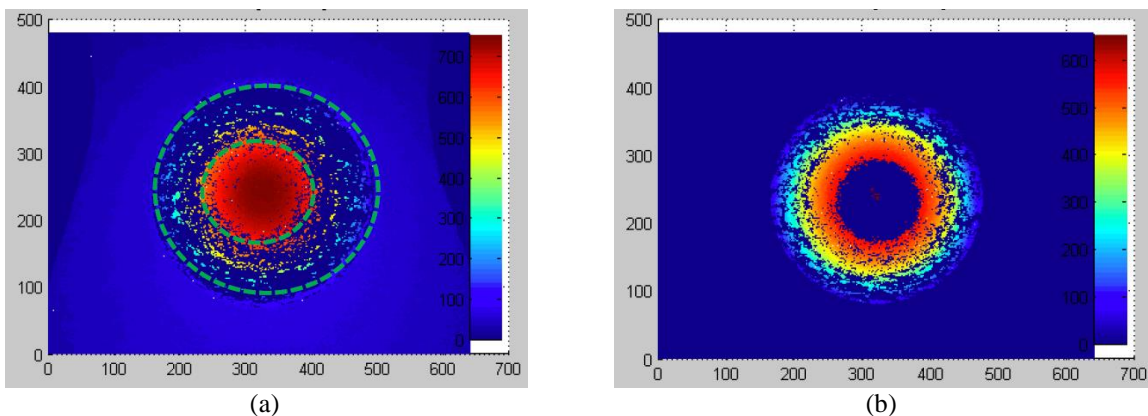
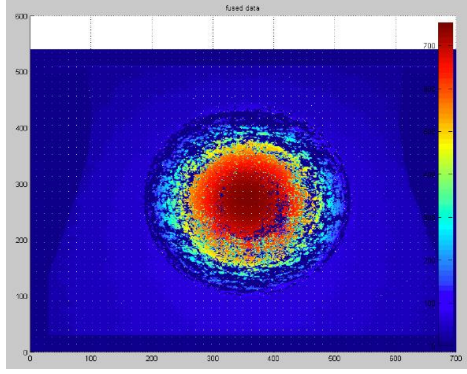


Figure 4. The uncertainty of the arithmetic mean fusion decreases given two independent datasets.





(c)

Figure 5. Individual measurement data of a sphere surface under 25 % (a) and 35 % (b) light intensity settings, and the fused result (c) [41].

2) Stitching

Stitching of surface measurement data has been used in interferometry since the 1990s [22,42], and is a typical case of data fusion. A large area surface can often not be measured by a single interferogram. Therefore, stitching of sub-aperture images to give a larger measuring area is an obvious solution. Figure 6 is a schema of a typical stitching interferometer. Stitching can be applied to most existing areal surface topography instruments [9], such as AFM, confocal microscopy or focus variation microscopy.

Stitching relies on a calibrated high-accuracy translation stage which is able to control the lateral movement of the sample at an accuracy level far below the pixel width. If the translation stage lacks control accuracy, the stitching is inexact and extra pre-stitching processes [43] (for example, pre-registration on the lateral plane or resampling) are needed, which increases the operational complexity. After the acquisition of a sequence of sub-aperture measurements at different regions, stitching is implemented.

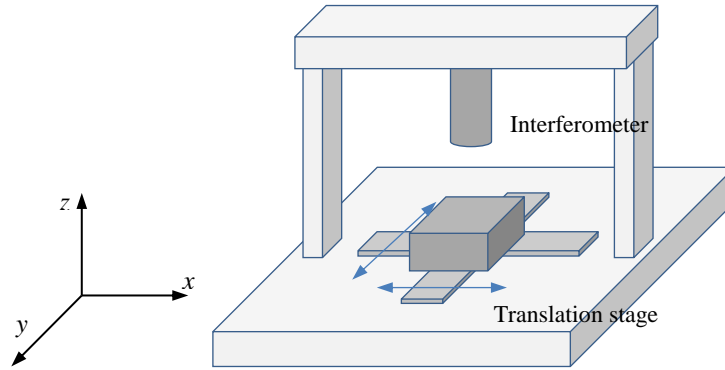


Figure 6. Sketch of a simple sub-aperture stitching interferometer.

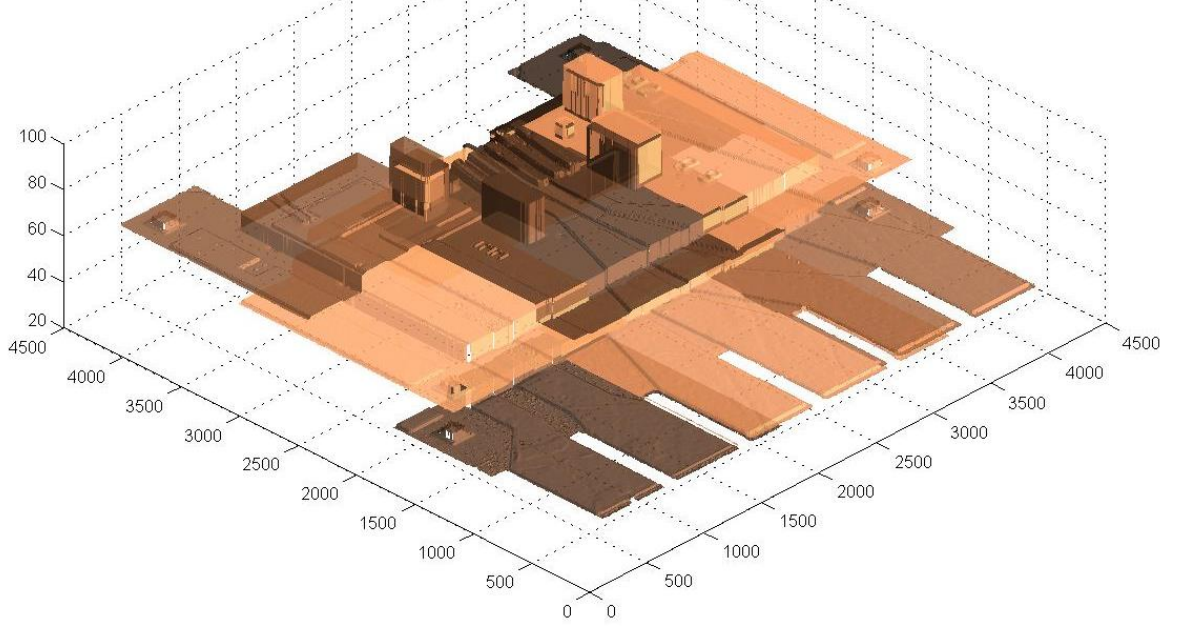
A typical stitching algorithm includes registration in three degrees-of-freedom, namely tip, tilt and piston [22], followed by a point-wise fusion process. The registration process superimposes extra offsets to each dataset on lower or higher orders [44], so that every individual spatial dataset can be described in the same coordinate system following the assumption:

$$\mathbf{z}_{ref}(x, y) = \mathbf{z}(x, y) + \Phi_{xy}\boldsymbol{\beta} + \boldsymbol{\varepsilon}, \quad (1)$$

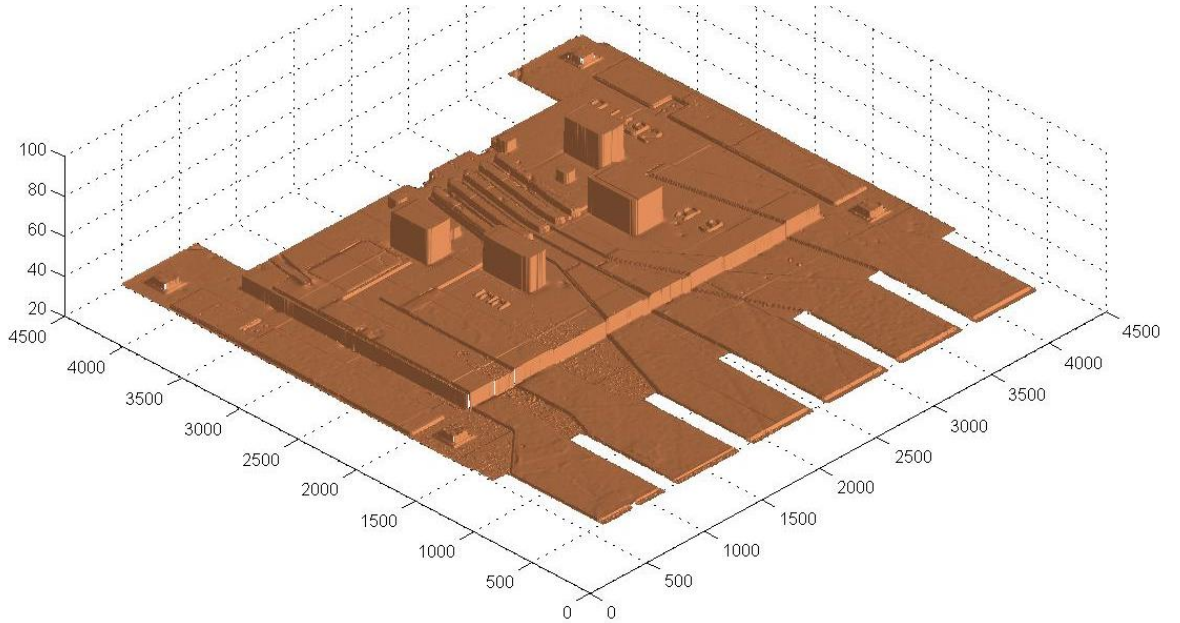
where $\mathbf{z}(x, y)$ is the vector of original sample values of an individual sample set, $\mathbf{z}_{ref}(x, y)$ is the vector of sample values of the same sample set but linearly transformed into the reference coordinate system, Φ_{xy} is the stitching error modelling matrix and $\boldsymbol{\beta}$ is the stitching parameter vector, $\boldsymbol{\varepsilon} \sim N(\mathbf{0}, \sigma^2 \mathbf{I})$. The main task of stitching algorithms is to estimate $\boldsymbol{\beta}$ for each individual sub-aperture measurement. Therefore, given $\mathbf{K} = \{1, 2, \dots, K\}$ sub-aperture images $\mathbf{z}_{k \in \mathbf{K}}$, by setting one as the reference, for example, \mathbf{z}_M , estimation of the stitching parameters $\boldsymbol{\beta}_{k \in \mathbf{K}, k \neq M}$ becomes the following minimisation problem

$$\boldsymbol{\beta} = \operatorname{argmin} \sum_{i \in K} \sum_{j \in K} \|\mathbf{z}_{inj} + \Phi_{inj} \boldsymbol{\beta}_i - \mathbf{z}_{jni} - \Phi_{jni} \boldsymbol{\beta}_j\|_2^2 \quad (2)$$

where $\boldsymbol{\beta}_M = \mathbf{0}$, $\Phi_{inj} = \Phi_{jni}$ and \mathbf{z}_{inj} denotes the vector of z -data of the i^{th} image corresponding to the j^{th} image. Once the registration process ends, fusion is implemented by simply taking the arithmetic mean of the sample values from each individual dataset at each overlapping position.



(a) Nine independent sub-aperture measurements (randomly coloured for visual discrimination) (unit: μm).



(b) The stitching result.

Figure 7. Stitching of nine sub-aperture measurements for an optical chip (unit: μm).

In Figure 7, an example of stitching for nine sub-aperture measurements is presented. In this example, an initial sub-aperture measurement in nine local regions was taken on an optical chip surface [45]. By using the near-origin local measurement in Figure 7a as the reference, the remaining eight datasets are registered and the fused result presents a usable measurement.

3) Range image fusion

Range image fusion, which deals with the fusion of resolution-inhomogeneous images, is an extension of general stitching. In range image fusion, the images to be fused can be from the same instrument with different (or the same) sensors, or from different instruments. Because there is no natural point-pair correspondence between overlapping datasets, a cross-resolution image registration algorithm and fusion algorithm need to be developed.

Research into range image fusion is limited, but see recent work by Ramasamy *et al.* [19,46]. In Ramasamy's framework, the inhomogeneous images are first resampled under the same sampling conditions. Then, a two-stage registration process is carried out: an initial coarse matching based on the sum of absolute differences or normalised cross-correlation [47], and a fine registration based on an iterative closest point algorithm [48]. In the fusion process, because input datasets usually have different uncertainty or information richness (measurement bandwidths), a weighted mean is normally taken. Ramasamy introduced some weighting methods from image processing techniques, including the regional energy [49], regional edge intensity [50] and the combination of wavelet coefficients and local gradients [51]. However, uncertainty propagation based on these weighting methods is currently unclear.

Theoretically, the choice of proper weights relies on the measurement uncertainties of each instrument. For example, given multiple images to be fused, and that have standard measurement uncertainties $\sigma_1, \sigma_2, \dots, \sigma_n$, an optimal design of weights $\mathbf{a} = [a_1, a_2, \dots, a_n]^T$ should minimise the standard uncertainty of the fusion result, *i.e.*

$$\operatorname{argmin}_{\mathbf{a}} \sigma_F^2 = \mathbf{a}^T V \mathbf{a}, \text{ subjected to } \|\mathbf{a}\|_1 = 1, \mathbf{a} \in [0,1]_n, \quad (3)$$

where, $V = \operatorname{diag}(\sigma_1^2, \sigma_2^2, \dots, \sigma_n^2)$. Therefore, the optimised weights for individual images can be calculated as

$$a_i = \frac{1}{\sigma_i^2 \sum \frac{1}{\sigma_j^2}}. \quad (4)$$

Under optimal weighting, the fusion result can always provide reduced uncertainty as

$$\min \sigma_F^2 = \frac{1}{\sum \frac{1}{\sigma_i^2}}. \quad (5)$$

In practice, the measurement uncertainty of individual images is usually unknown or inaccurate, especially when resampling is implemented in pre-processes [19,46], therefore, the theoretical weight design may not be optimal.

4) Point cloud fusion

Point cloud fusion includes the fusion of spatial data in point cloud forms, which can be widely found in statistical analysis [52]. Because any other spatial data forms can be represented in point cloud forms, point cloud fusion is becoming an important research topic in surface metrology, especially in dimensional metrology [1]. Surface measurement data in point cloud forms can normally be found on CMM systems or other dimensional metrological systems. Unlike images, which have regular grid data forms and can be efficiently modelled by tensor-product models, point cloud data usually needs relatively complex mathematical representation and analysis. For example, radial basis function (RBF) modelling has the typical computational complexity of the order of $O(mn^2)$ [53], compared to $O(2mn)$ with efficient tensor-product methods, where m and n are the number of data points and number of RBF centres respectively.

Registration of point cloud data into a common coordinate system is usually the first task before the fusion of data. Many algorithms for point cloud registration have been developed, such as the iterative closest point algorithms for fine registration [48,54,55] and diverse signature-based rough registration algorithms [56-58].

Registration guarantees the individual datasets are represented in the same coordinate system so that they can be fused.

After registration, fusion is carried out to combine the datasets in each overlapping region so that an enhanced output is produced. Currently, most point cloud fusion algorithms convert 3D problems into 1D problems, by projecting a 3D point cloud onto a reference surface so that the 3D geometry can be described by surface height z as a function of x and y coordinates, *i.e.* $z = f(x, y)$. Thus, fusion of x , y and z data can be reduced down to fusion of z data only. Typical point cloud fusion algorithms include hierarchical Gaussian process fusion and its derivatives [59-63]. These Gaussian process-based fusion methods approximate the residuals between two reliability-differentiated datasets using Gaussian process models. The uncertainty propagation for such fusion solutions is still not clear.

There are other fusion algorithms available for point cloud data, such as Kalman filter methods based on parametric approximation [64]. All these algorithms for point cloud fusion rely on different approximation techniques, such as B-splines and Gaussian process approximation [53,65,66]. A review of these detailed algorithms is given in section 4.

3. Common issues in fusion processes for spatial data

Among the applications of spatial data fusion, the complexity of input data forms increases, from repeated measurements, to stitching, range image fusion and point cloud fusion (see Figure 8). Fusion of simpler forms of input data can, therefore, usually be implemented using the algorithms for complex forms of data. For example, repeated measurement fusion does not require registration. A stitching algorithm can hence be applied to repeated measurements but with the registration process omitted. Table 1 shows the main registration and fusion methods used for different spatial data fusion applications, in which it can be observed that the complexity of algorithms increases, as shown in Figure 8.

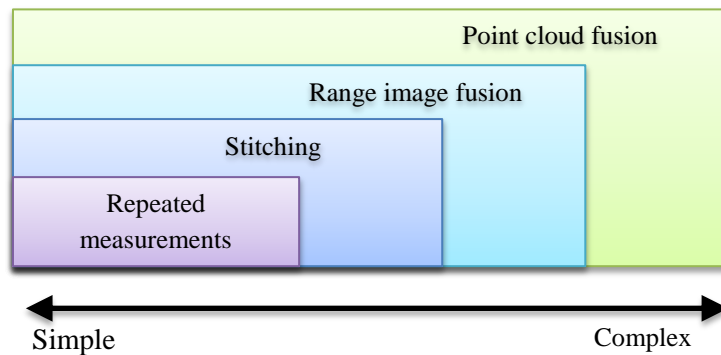


Figure 8. Scopes of spatial data fusion methods.

Table 1. Different methods of spatial data fusion and their corresponding registration and fusion methods.

Fusion \ Registration	Simple mean (min/max)	Weighted average	Approximated fusion
NA	Repeated measurements		
3DoF registration	Stitching		
5~6DoF registration		Range image fusion	Point cloud fusion

In spite of the differences, there are some common processes among the fusion methods. In most situations, the sequence of complete fusion processes for spatial data includes [1,19]:

- pre-processes (denoising, downsampling, *etc.*),
- registration,
- fusion, and
- post-processes (data reduction, rendering, spatial database management, *etc.*).

In this section, some common issues in the above list of processes for surface measurement are discussed.

3.1. Data forms

Diverse forms or formats of data can be found in surface metrology. These different forms of data can represent different types of geometry and have different levels of computational complexity. Table 2 summarises the typical forms of data found with surface measuring instruments, where x D implies that a dataset has full x degrees-of-freedom in the x -dimension; $x.5$ D implies that a dataset has $x + 1$ dimensions in total, with one dimension of data being a function of the other x dimension's data. For example, 2.5D means that a dataset has three dimensions in total, but one dimension's information is a dependent variable of the other two dimensional variables.

Fusion algorithms for different forms of data are different. For example, the sum of absolute difference-based registration [47] is only applicable to images. Iterative closest point registration is only applicable to point cloud data [67]. In the fusion of mixed forms of data, there should be a common form of data which is computationally convenient in the processes of registration and fusion, and can be easily converted to other forms of data.

The convertibility between these data forms is presented in Figure 9, in which, the data processing speed increases for the data forms from left to right. In Figure 9, the green arrows indicate a direct conversion is available with a small number of, or zero, operations; the red arrows indicate that the conversion needs algorithms, such as projection [68], interpolation [65,69-71] or iso-surface extraction [72,73]. Among the different forms of data, point clouds can be seen as the most popular form to which other forms of data can conveniently be converted. Therefore, point clouds are recommended as a common form of data for the fusion of mixed forms of spatial data.

Table 2. Different data forms found in surface measurement.

Level	Name	Data storage	Instrument applications	Surface function models	Complexity in linear modelling
5	3.5D volume data	$[V]_{K \times L \times P (KLP=N)}$	CT	Iso-surface to be extracted out	Highly complex
4	3D point cloud	$\begin{bmatrix} X \\ Y \\ Z \end{bmatrix}_N$	CMM	$x_n = f_x(u_n, v_n),$ $y_n = f_y(u_n, v_n),$ $z_n = f_z(u_n, v_n).$	$O(3P(m^2N))$
3	3D grid data	$\begin{cases} [X]_{K \times L} \\ [Y]_{K \times L} \\ [Z]_{K \times L} \end{cases}_{(KL=N)}$	CMM	$x_{k,l} = f_x(u_{k,l}, v_{k,l}),$ $y_{k,l} = f_y(u_{k,l}, v_{k,l}),$ $z_{k,l} = f_z(u_{k,l}, v_{k,l}).$	$\leq O(3P(m^2N))$
2	2.5D scattered data	$\begin{bmatrix} X \\ Y \\ Z \end{bmatrix}_N$	CMM	$z_n = f(x_n, y_n),$ $n = 1, \dots, N.$	$O(P(m^2N))$
1	2.5D profile set	$\begin{cases} [Z]_{N_1} \\ [Z]_{N_2} \\ \vdots \\ [Z]_{N_K} \end{cases}_{(\sum N_k=N)}$	Stylus	$z_{k,n_k} = f(x_k, y_{n_k})$ $k = 1, \dots, K,$ $n_k = 1, \dots, N_k.$	$\leq O(P(m^2N))$
0	2.5D range image	$[Z]_{K \times L (KL=N)}$	CSI, AFM, SL scanner, FV, confocal, stylus	$z_{k,l} = f(x_k, y_l),$ $k = 1, \dots, K,$ $l = 1, \dots, L.$	$\leq O(P(m^2N))$

Note: $P(\cdot)$ denotes the algorithm complexity of matrix multiplication, m is the number of modelling parameters, N is the data size.

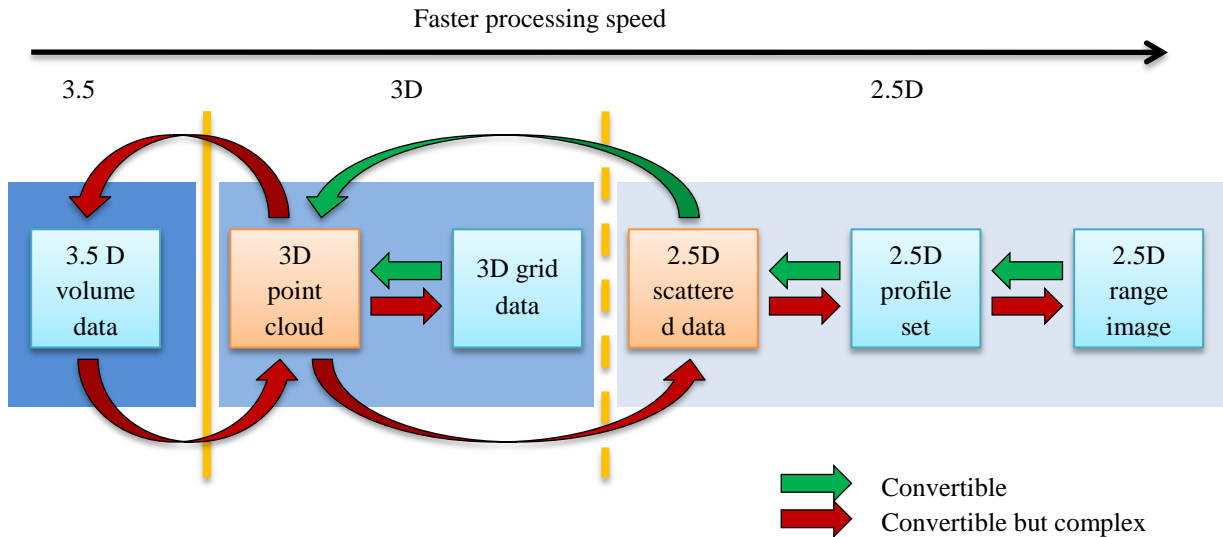


Figure 9. The convertibility between different forms of data.

3.2. Pre-processes

1) Levelling rotation

For the fusion of point clouds, levelling rotation [74] is an optional step before registration. The coordinate system of a dataset is rotated so that the surface points lie approximately horizontally. In this way, surface samples can be modelled explicitly by $z_i = f(x_i, y_i)_{i=1, \dots, N}$. Surface data with re-entrant features needs complex fusion algorithms, which are beyond the scope of many of the existing fusion solutions introduced in section 4.

2) Filling missing data

In range image fusion, missing data should be replaced by neighbouring sample values or other meaningful values [75], for example, zero, or min/max values, to avoid later computation failures. However, not all existing algorithms fail for images with missing data. Filling missing data is, therefore, an optional procedure which is not recommended when there are concerns about the reliability of fusion.

3) Removing outliers

Due to effects of the measurement environment, outliers can exist and they vary a lot in shape depending on different sensing methods. Registration of outlier-contaminated datasets produces registration errors. The registration-induced errors can be magnified in the final fusion results. Therefore, outliers must be identified, and removed or corrected [76].

4) Denoising

Noise, such as white noise and pink noise, can be found in any measurements. There are some mature algorithms developed for computational efficiency with range images, such as least-squares spline methods, total variation-minimisations [77,78] and algorithms for higher dimensional data [75]. Currently, advanced algorithms, such as L1 spline methods, are under development, which can avoid oscillations for abrupt change signals and are insensitive to outliers [79,80].

Denoising as a pre-process is optional because many registration [48] and fusion [62] processes are insensitive to noise. In some fusion methods, denoising is included in the fusion process, such as in Gaussian process fusion [63].

3.3. Registration

All fusion methods for spatial data, except repeated measurements, need a registration process to linearly transform different datasets to the same coordinate system before fusion (see Figure 10). Practical registration processes usually proceed in an initial coarse registration and are followed by a fine registration. The former process globally searches for a rough registration position which speeds up the latter fine registration and avoids the whole registration failing by being trapped at a local optimisation point.

1) Coarse registration

Coarse registration aims to initially place a dataset in the same coordinate system as a design (template) model or another dataset. Many methods have been developed for this purpose, most of which efficiently conduct the task by simply matching a set of fiducial marks or points, instead of using all the sample points [56-58,81,82]. For coarse registration of range images, the sum of absolute differences and normalised cross-correlation [47] are usually efficient solutions [41].

2) Fine registration

Fine registration usually applies to all the sample points to determine final registration parameters by minimising the distance between two sets of data. Fine registration provides the six parameters $[t_x, t_y, t_z, \alpha, \beta, \gamma]$ for output, which respectively denote the relative translations and rotations on/around the x -, y - and z -axes.

Iterative closest point (ICP) algorithms [48,54,55] are a set of widely preferred methods for fine registration. ICP algorithms search for the corresponding closest points from a dataset for each sample point of a template (or another dataset), and then calculate registration parameters for the established correspondence relationship, iteratively until a condition is achieved. The selection of an appropriate closest point searching algorithm usually determines the registration accuracy. Typical closest point searching methods include brute-force search, Delaunay triangulation and kD-tree methods [83]. For surface measurement data, with numbers of sample points that is usually in the thousands, kD-tree is normally the recommended method due to its high computational efficiency. Once a point-correspondence relationship is established, calculation of the registration parameters can be implemented in a least-squares manner, for example, based on singular value decomposition [68] or quaternions [84]. Further details on ICP algorithms can be found elsewhere [67].

For very dense input datasets, downsampling is usually implemented to speed up registration computations [67]. The selected downsampling methods influence the accuracy of registration and hence the accuracy of the final fusion. Simple random downsampling [85] has been shown to be unbiased to the prediction of registration parameters. Other intelligent sampling [86] methods are expected to improve the convergence rate [87] by densely reserving sample points at the feature-rich regions. The features can include peaks, pits, saddle points and feature edges. For example, intelligent sampling by adapting sample points to surface curvatures [67] has been demonstrated to improve the registration accuracy and speed.

3.4. Fusion

1) Preparation of data for fusion

As described in section 3.1, fusion of mixed forms of data is expected to be carried out under a common data form, for example, point clouds. For the data in point cloud forms, a further conversion to scattered data forms is needed to simplify 3D fusion problems to fusion of z data only.

Data fusion should be carried out on the data points within the overlapping areas between two or multiple datasets. The peripheral points outside the overlapping areas should be removed for computational efficiency. In-hull indexing algorithms [88] can be employed for this purpose by respectively applying one dataset as the

template hull and searching for the data points of other datasets within the hull. Figure 10 shows the role of in-hull indexing.

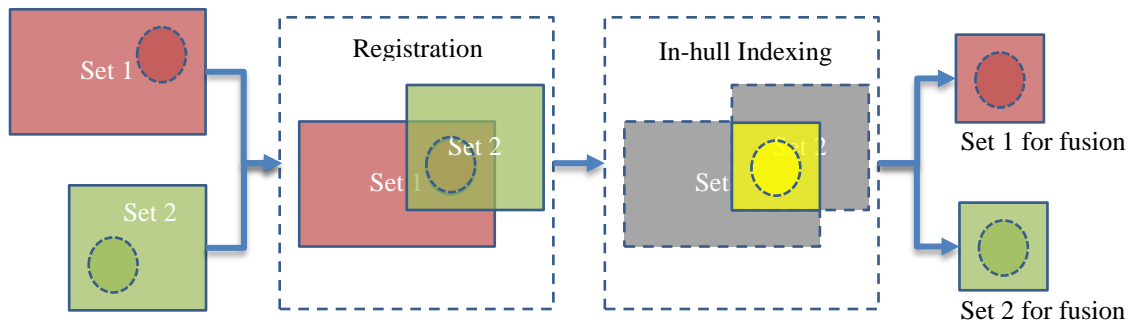


Figure 10. Schema of the effects of registration and in-hull indexing.

2) Fusion of data

For simple data fusion solutions, such as repeated measurements, stitching and range image fusion, fusion of data is implemented by averaging (simple mean or weighted mean) each pair of correspondent points in a point wise manner from individual sets of data. For point clouds or scattered data, different datasets usually have varied sampling conditions, which indicate that there is usually no naturally existed point-correspondence relationship. Therefore, fusion of point clouds or scattered data needs advanced algorithms.

Currently, most fusion solutions for point clouds rely on appropriate surface fitting techniques. For example, in references [60,62,63], Gaussian process-based surface fitting techniques are used to approximate the residuals between each pair of input datasets. Other fitting techniques, such as B-spline wavelets-based [89,90] surface approximation techniques, may also provide good fusion results.

Another classical fusion technique for point clouds is weighted least-squares fusion based on parametric linear fitting [91]. Linear fitting ensures the fusion is simplified for uncertainty control and fast for numerical computation. However, flexible and robust fitting models are difficult to construct for practical signals, especially signals with abrupt changes. Therefore, there has only been limited work in dimensional metrology on linear fitting. Despite the difficulty of fitting, weighted least-squares fusion can be applied for smooth surfaces, which can be efficiently approximated using many common fitting models [53].

In section 4, detailed mathematical descriptions of the two methods, *i.e.* residual fitting-based fusion and weighted least-squares fusion, are given.

3.5. Post-processes

There are normally three post-processes for data fusion, including data reduction, storage and rendering, with the assistance of a spatial database management system.

Once a fusion result is obtained, the original datasets become redundant and can be abandoned. However, from the concern of traceability, the redundant data points may need to be reserved for further validation of the fusion reliability. Also, fusion results are usually in the form of a parametric or non-parametric model that can be directly saved as a set of model parameters (encoding) or a set of designed samples drawn from the fused model. Storage in the form of model parameters is usually efficient (small in memory size), but requires a variety of model-predicating algorithms (decoding) to render the fusion results in a Cartesian space. Storage in a set of extracted samples may be larger in size, but has the consistent form of expression as the unfused data in the peripheral areas (as in Figure 10). Such homogeneous outputs simplify the computational requirement for the tools of data communication and rendering. In summary, fusion results can be saved as a slimmed-down version with the model parameters, or a medium-sized version with a designed sample set extracted from the fused model, or a full version with all the original data preserved. The medium-sized

version, with appropriate sample design, can be set as a default output due to its merits on storage space and management.

Rendering of fusion outputs relies on the development of a fast and user-friendly interface. In this interface, rendering of all fused datasets in a specific field of view is not necessary due to the limitations of the computation speed. An indexing process is needed instead to select the relevant datasets for a given field of view. The indexed datasets for a field of view should only include the datasets sampled from the top surfaces for a specific field of view. When rendering fused results in the form of 3D point clouds, the indexing needs more complicated solutions than range images in which the indexing proceeds only in a 2D plane. Meshing [92,93] of point clouds is another requirement for rendering. A meshing process, for example Delaunay triangulation [69], finds the neighbouring points for any point in a cloud, by which a set of discrete spatial points can be rendered as closely connected small facets. Meshing-based rendering can express real-world entities in a visually friendly manner.

With the exception of the main post-processes described above, there are other processes users may need, such as measurement (for example, measuring the distance between two spatial points), editing (for example, adding or removing a data point or other types of geometry) and analysis [94]. All these post-processes are carried out based on a specialised spatial database management tool. Different from any existing database management systems in surface or dimensional metrology, this spatial data management tool should be able to effectively process large data. For example, an automated measurement of a large area surface by stitching hundreds to thousands of sub-aperture range images may produce a file of gigabytes or more. Manipulation of such large file may easily suffer from slow processing and large memory requirements.

4. Spatial data fusion algorithms

Repeated measurements, stitching or range images use simple or weighted means [19] as the fusion solutions. Fusion of point clouds needs advanced fusion solutions. Some existing fusion solutions for data in the form of point clouds rely on advanced surface fitting techniques, by either fitting the source surface signal or the residuals between two independent datasets with some common models. In this section, some promising fusion algorithms for spatial data in point cloud forms are discussed.

4.1. Weighted least-squares fusion

Weighted least-squares fusion is a classical fusion technique relying on parametric linear fitting [91] of source surface signals. Given a linear measuring system,

$$\mathbf{z} = H\mathbf{x} + \boldsymbol{\varepsilon}, \quad (6)$$

where \mathbf{x} is a n -vector comprised of the model parameters to be measured, H is a $m \times n$ ($m > n$) model basis function matrix (or measurement matrix), \mathbf{z} is a m -vector of the measurement results, $\boldsymbol{\varepsilon}$ is a normal and independent and identically-distributed noise vector with $\boldsymbol{\varepsilon} \sim N(\mathbf{0}, \sigma^2 \mathbf{I})$. Such linear systems can approximate most practical surfaces, with an appropriate design of the measurement matrix. With multiple and independent measurement results from different instruments for the same object, say $\{\mathbf{z}_k \in \mathbb{R}^{m_k}\}_{k \in K}$, with the noise levels $\boldsymbol{\varepsilon}_k \sim N(\mathbf{0}, \sigma_k^2 \mathbf{I})$, the model parameter vector \mathbf{x} of the object can be estimated by minimising the cost function

$$\sum_{k \in K} w_k \|\mathbf{z}_k - H_k \mathbf{x}\|^2, \quad (7)$$

where w_k is a designed weight for each dataset. By setting the weights $w_k = \frac{1}{\sigma_k^2}$, the best linear unbiased estimation (BLUE) of the model parameters can be achieved, which has the minimum variance [91], *i.e.* the minimum evaluation uncertainty in this case.

The minimisation can be achieved by forcing the partial differential of the function (equation (7)) to α equal to $\mathbf{0}$. Hence, the weighted least-squares fusion for the estimation of the model parameter \mathbf{x} has the form

$$\hat{\mathbf{x}} = (H^T W H)^{-1} H^T W \mathbf{z}, \quad (8)$$

where $H = \begin{bmatrix} H_1 \\ H_2 \\ \vdots \\ H_K \end{bmatrix}$, $W = \text{diag}(W_1, W_2, \dots, W_K)$ with $W_k = \text{diag}(w_k, w_k, \dots, w_k)_{m_k}$, and $\mathbf{z} = \begin{bmatrix} \mathbf{z}_1 \\ \mathbf{z}_2 \\ \vdots \\ \mathbf{z}_K \end{bmatrix}$.

The prediction output and its variance of the fused model vary at different observation positions [53]. However, a typical prediction of the model output can usually be obtained at the observation positions, which are the same as all the individual measurement datasets, *i.e.*

$$\hat{\mathbf{z}} = H \hat{\mathbf{x}} = H(H^T W H)^{-1} H^T W \mathbf{z}. \quad (9)$$

The following shows that such a typical prediction has a minimum variance compared to the predictions based on any individual dataset only.

Since the prediction error $\hat{\mathbf{r}} = \hat{\mathbf{z}} - H \mathbf{x}$ has the covariance

$$V(\hat{\mathbf{r}}) = H(H^T W H)^{-1} H^T = W^{-1/2} Q_{w1} Q_{w1}^T W^{-1/2}, \quad (10)$$

where $V = W^{-1} = W^{-1/2} W^{-1/2}$ and $W^{1/2} H$ has the QR factorisation as $W^{1/2} H = Q_w R_w = Q_{w1} R_{w1}$. The squared standard prediction uncertainty, *i.e.* the mean squared error of the prediction in equation (9), can be expressed as

$$\begin{aligned} u^2(\hat{\mathbf{z}}) &= \text{MSE}(\hat{\mathbf{z}}) = \frac{1}{\sum_{k \in K} m_k} \text{tr}(V(\hat{\mathbf{r}})) \\ &= \frac{1}{\sum_{k \in K} m_k} \sum_{k=1, \dots, K} \left(\frac{1}{w_k^2} \sum_{i=1+\sum_{s=1, \dots, k-1} m_s}^{\sum_{s=1, \dots, k} m_s} \sum_{j=1}^n q_{i,j}^2 \right) \\ &\approx \frac{n}{\sum_{k \in K} \frac{m_k}{\sigma_k^2}} \end{aligned} \quad (11)$$

where $q_{i,j}$ are the entries of Q_{w1} . By substituting K by 1 in the equation (11), the squared standard prediction uncertainty of the least-squares fitting of each individual dataset without fusion can be obtained as

$$u^2(\hat{\mathbf{z}}_i) = \frac{n}{m_i} \sigma_i^2. \quad (12)$$

Therefore, it can be easily shown that $u^2(\hat{\mathbf{z}}) < u^2(\hat{\mathbf{z}}_i)$, *i.e.* the fused result always has a smaller prediction uncertainty than that without fusion.

The weighted least-squares fusion described above is well known for its advantage in fast computation. However, if new sets of sample data are dynamically added in, the fusion result has to be updated by involving all previous datasets. A Kalman filter [23, 64] provides an alternative execution algorithm to the weighted least-squares fusion, by successively integrating new datasets with previously fused results, without reference to every previous set of data [64].

The difficulty of weighted least-squares fusion is that it requires a good design or measurement model to approximate the source surface. For surfaces with an unknown design model, or if the manufacturing error is large, some common models with a high degree of flexibility can be used for general fusion purposes. Typical common models include diverse B-spline models with different knot settings [65,89,90,95], which can

approximate general smooth signals well. For signals with abrupt changes in geometry, weighted least-squares fusion may not be recommended because the fitting solutions for such complex geometries are usually not available.

To the authors' knowledge, there is a lack of experimental research on weighted least-squares fusion for surface measurement. As an inspiring example, Figure 11 presents the fusion results of two uncertainty-distinct datasets from a cubic B-spline curve, with the knots set at $[-0.5, -0.4, 0, 0.4, 0.6]$, with 2000 random simulations. Within every simulation, the measurement noise is randomly generated. This simulation shows a steady reduction of the estimation error by approximately 1/10 from that of the individual set with the smaller estimation error.

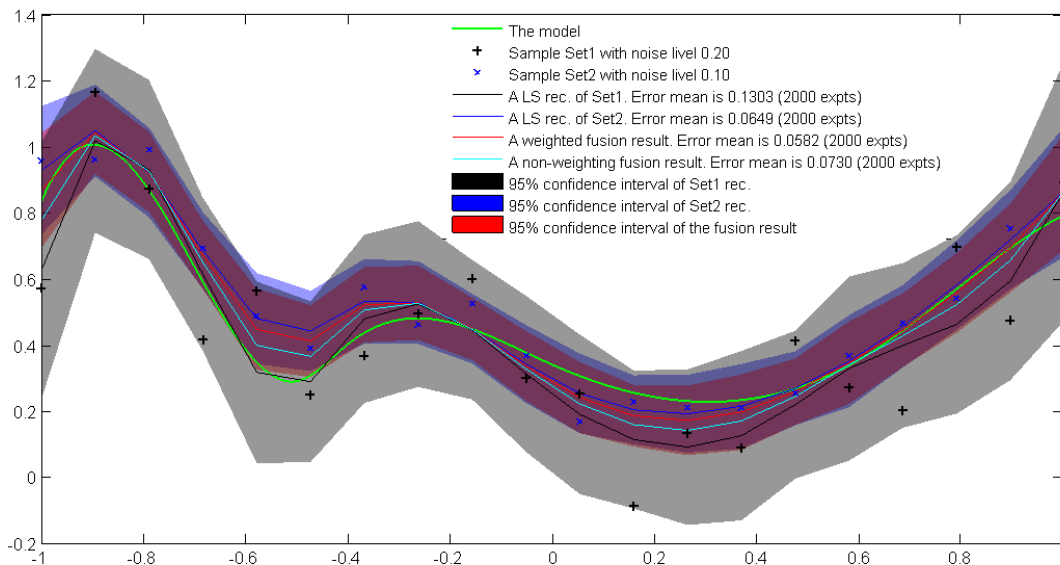


Figure 11. Simulation of the effect of the weighted least-squares fusion.

Another application difficulty of weighted least-squares fusion is derived from the calculation of the weights. Because the optimised weights are the reciprocal of the standard measurement uncertainty of each individual dataset, the reliability of the knowledge about the individual measurement determines the accuracy of fusion. However, the information about each individual measurement is usually fuzzy due to variable environmental conditions. Therefore, the feasibility of weighted least-squares fusion in practical situations has not been satisfactorily demonstrated.

4.2. Residual approximation-based fusion

Residual approximation (RA)-based fusion is a fusion solution which applies approximation to the systematic offset (residuals) between two individual datasets from different sensors. An analytical expression of the uncertainty propagation of the RA-based fusion methods is currently unavailable. However, many existing simulations have shown that such methods can provide uncertainty-reduced fusion results when compared with those from any individual set. As a competitive solution to weighted least-squares methods, RA-based fusion can be applied effectively for both smooth and non-smooth signals.

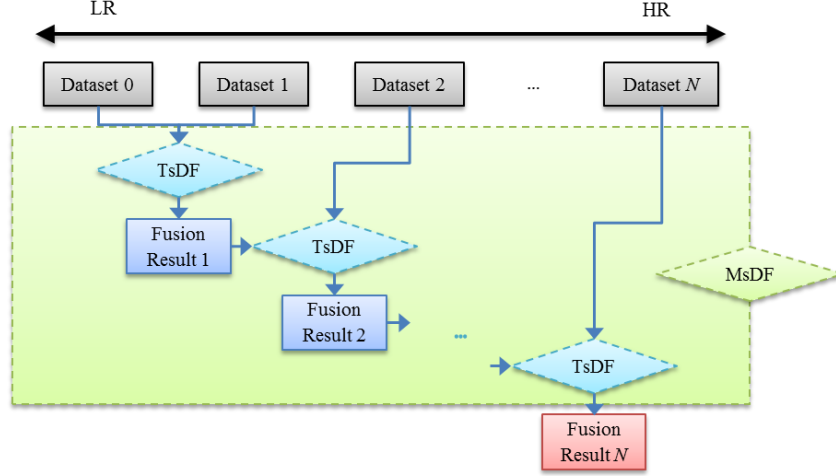


Figure 12. Schema of two-sensor data fusion for multi-sensor data fusion.

RA-based multi-sensor data fusion proceeds in an ordered sequence with a common fusion process for every two sets of data; a process known as two-sensor data fusion [96]. As shown in Figure 12, individual datasets are first ordered according to their reliability level ranking. Then, from the dataset with the lowest reliability, RA-based fusion is carried out for each dataset with the previously fused result (or dataset), until all the input data are integrated. If there is no difference in the uncertainty for input datasets or the datasets are ranked inappropriately [60], the performance of RA-based fusion is uncertain.

1) Gaussian process fusion

A typical RA-based fusion method is Gaussian process (GP) fusion, which links two datasets by approximating their residuals as a GP function [59,61,62]. GP approximation is a non-parametric fitting method [66]. Given a set of residual data (\mathbf{x}, \mathbf{y}) , with $\mathbf{x} \in \mathbb{R}^d$, a GP model, which is determined by a hyper-parameter set $\boldsymbol{\theta}$, can be trained by maximising the marginal likelihood function (usually expressed in logarithmic form):

$$L = \log \mathbf{P}(\mathbf{y}|\mathbf{x}, \boldsymbol{\theta}) = -\frac{1}{2} \log |V_{\boldsymbol{\theta}}| - \frac{1}{2} (\mathbf{y} - \boldsymbol{\mu}_{\boldsymbol{\theta}})^T V_{\boldsymbol{\theta}}^{-1} (\mathbf{y} - \boldsymbol{\mu}_{\boldsymbol{\theta}}) - \frac{n}{2} \log(2\pi), \quad (13)$$

where $V_{\boldsymbol{\theta}}$ is the covariance matrix defined by the sample points \mathbf{x} and the hyper-parameters $\boldsymbol{\theta}$, and $\boldsymbol{\mu}_{\boldsymbol{\theta}}$ is the mean vector defined by $\boldsymbol{\theta}$. The optimisation problem in equation (13) can be solved by using many well-known algorithms, such as diverse interior-point methods [97] and trust-region-reflective methods, using MATLAB [98]. Another effective minimisation algorithm can be found in the GPML toolbox [99]. Once the hyper-parameters are optimised, the fitting prediction values \mathbf{y}_* can be calculated based on the posterior Gaussian model

$$\mathbf{y}_* | \mathbf{y} \sim N(\boldsymbol{\mu}_* + V_*^T V^{-1} (\mathbf{y} - \boldsymbol{\mu}), V_{**} - V_*^T V^{-1} V_*), \quad (14)$$

where V is the covariance matrix defined between the sample positions of the training dataset and themselves, V_* is the covariance matrix defined between the sample positions of the training dataset and the prediction positions, V_{**} is the covariance matrix defined between the prediction positions and themselves, $\boldsymbol{\mu}$ and $\boldsymbol{\mu}_*$ are respectively the mean value (usually the predictions from previously fused result or another dataset with lower reliability, in GP fusion) vectors on the sample positions of the training dataset and the prediction positions. In short, the prediction and prediction variances can be efficiently computed by the linear system in equation (14).

Given two sets of input data, with one as the high reliability (HR) set \mathbf{z}_1 and the other as the low reliability (LR) set \mathbf{z}_2 , GP fusion links the two datasets by approximating the residuals of the two datasets as a GP function. For example, a typical fusion model [60] has the form of

$$\begin{aligned}
z_1(x_i, y_i) &= \beta(x_i, y_i)\hat{z}_2(x_i, y_i) + \delta(x_i, y_i) + \varepsilon_1, \varepsilon_1 \sim N(0, \sigma_1^2), \\
z_2(x_i, y_i) &= \hat{z}_2(x_i, y_i) + \varepsilon_2, \varepsilon_2 \sim N(0, \sigma_2^2), \\
\beta(x_i, y_i) &= \beta_0 + \beta_1 x_i + \beta_2 y_i, \\
\delta &\sim GP(m_r, k_{l_r, \sigma_r^2}),
\end{aligned} \tag{15}$$

where \hat{z}_2 is a fitted (or denoised) version of the LR set z_2 , with $\hat{z}_2 \cong z_2$, δ , defined by the mean function m_r and the covariance function k_{l_r, σ_r^2} , is the GP linkage function which describes the systematic offset between the two input datasets, β is a rescaling function which reduces the scale offset between the two input datasets, and ε_1 and ε_2 are white noise. β can be substituted by other polynomial functions. However, it has been claimed [8] that a simple 1st degree polynomial rescaling is flexible enough for most practical cases. β can simply be set as unity if there is no scale bias between \mathbf{z}_1 and \mathbf{z}_2 . Based on the linkage model in equation **Error! Reference source not found.**, the fusion result can be expressed by a composition of the denoised LR data and the GP linkage function:

$$z_F = \beta(x_i, y_i)\hat{z}_2(x_i, y_i) + \delta(x_i, y_i). \tag{16}$$

The fitting method for the LR set in equation (15) is free to be defined. Different constructions of the LR model \hat{z}_2 influence the reliability of the later GP fusion. For example, \hat{z}_2 can be another GP model with $\mathbf{0}$ as the mean, *i.e.*

$$\hat{z}_2(x_i, y_i) \sim GP(\mathbf{0}, k_{l_2, \sigma_2^2}). \tag{17}$$

The $\mathbf{0}$ -mean GP model can provide a flexible approximation for smooth signals [66]. By combining the fitting models in equations (15) and (17), a hierarchical GP model is constructed, which is also called the Bayesian hierarchical Gaussian process [60,62]. \hat{z}_2 can also be approximated by using some linear models, *i.e.*

$$\hat{z}_2(x_i, y_i) = \mathbf{C}\boldsymbol{\alpha}, \tag{18}$$

where \mathbf{C} is a design matrix and $\boldsymbol{\alpha}$ are the modelling control parameters. Many mature linear interpolation and smoothing algorithms can be applicable to linear fitting, including diverse spline methods and Delaunay triangulation-based interpolation methods [65,69-71,89,100]. In simplified cases, for example in which \mathbf{z}_1 and \mathbf{z}_2 have the same sample positions or the sample noise is relatively small, \hat{z}_2 can simply be substituted by the source data \mathbf{z}_2 . The linear approximation given by equation (18) and the simple replacement by the source data are computationally efficient when the data size is too large.

2) Other fusion models

Approximation of the residuals between any two sets of data can also be implemented by using other models, either, parametric or non-parametric. Because the input datasets usually have different sizes, a flexible and efficient approximation method must be found, for which the fusion accuracy is insensitive to data size. A typical such approximation method is multilevel B-spline approximation (MBA) [89]. MBA predicts at a location far from the available input data points as 0 in default and works stably with any size of a dataset. Such stability means that MBA is a promising fusion solution.

MBA provides an approximation of a source surface with a sum of multiple model surfaces at different resolution levels, *i.e.*

$$\mathbf{z} = \mathbf{z}_0 + \mathbf{z}_1 + \dots + \mathbf{z}_K, \tag{19}$$

where $\mathbf{z}_k \in S_k$ and $\{S_k\}$ is a nested sequence of subspaces with $S_0 \subset S_1 \subset \dots \subset S_K$. For example, given a set of sample points within a square domain, $\Omega = [0, m] \times [0, n]$. A hierarchy of control lattices $\{\Phi_k\}_{k=0,1,\dots,K}$ can be designed overlaid on the domain Ω with $(2^k + 3) \times (2^k + 3)$ control points, based on cubic B-splines [95].

By assigning the maximum approximation level K , MBA proceeds by iteratively estimating the parameters of each level of control lattice in a weighted and least-squares sense. Then, *via* an appropriate reconstruction algorithm, for example, knot refinement [95], the original surface can be simply fitted (smoothed or interpolated) and predicted through a linear system at any desired position.

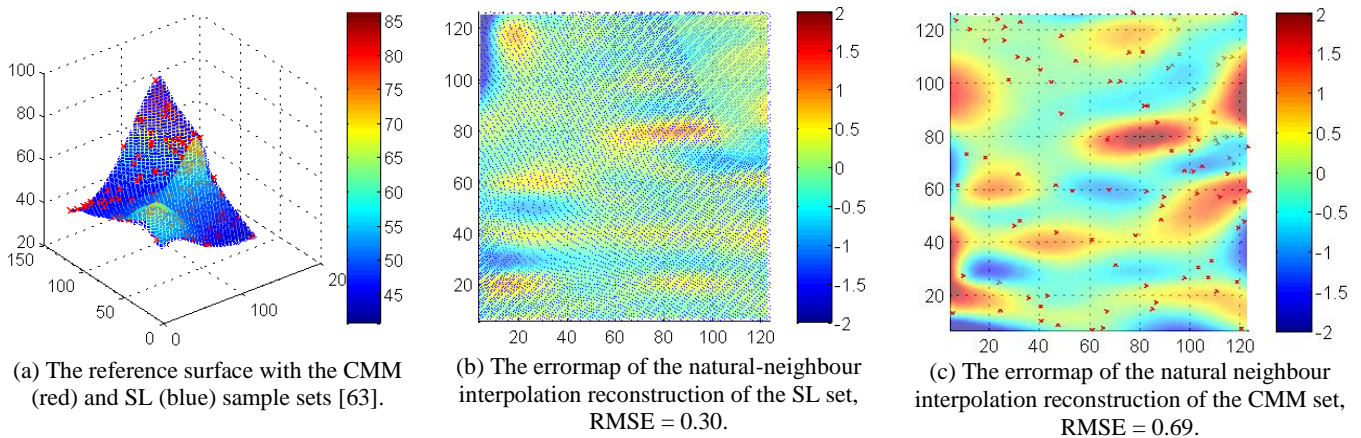
Other approximation models include regular grid or non-regular grid B-spline fitting models [65,95], radial basis function models, Fourier series models and wavelet models [53]. However, these models do not have such stable characteristics as the MBA method. Therefore, the feasibility of these alternative models for practical fusion is unclear and needs validation.

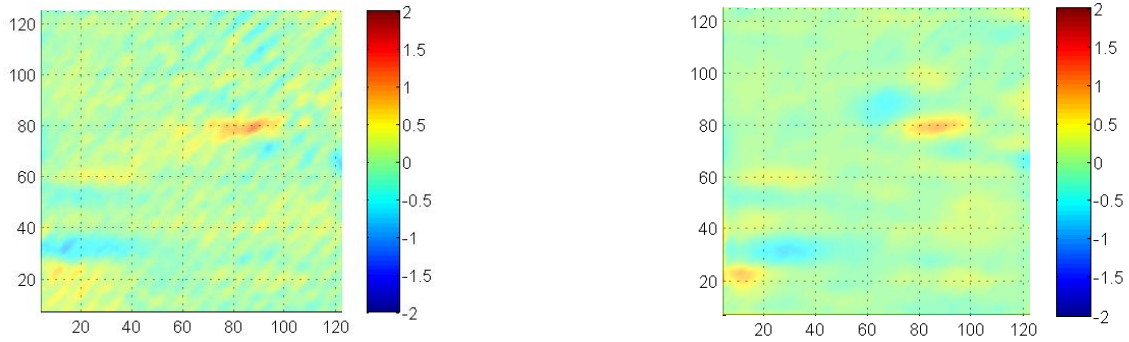
3) Discussion

RA-based fusion methods, especially GP fusion, are well-behaved fusion methods which have been demonstrated with experiments and simulations [60,62,63]. GP fusion, which uses one dataset as the mean and approximates the residuals between the dataset and another using a GP model, effectively avoids miscellaneous design of the parametric models for a complex surface.

From a statistical standpoint, a prediction based on a HR set solely can be understood as a posterior estimation with null prior; GP fusion can be understood as a posterior estimation with a rough prior estimate based on a LR set. Therefore, with a prior estimate, RA-based fusion may have a high probability to provide improved fusion results with reduced uncertainty. For smooth (with small maximum local curvature) signals, a rough prior estimate may contribute insignificantly. But for non-smooth (with abrupt changes) signals, a rough prior estimate influences the fusion result with a higher weight than the HR dataset, especially when predicting at the observation positions near abrupt change areas. In addition, for the situations when a HR dataset is dense, a rough prior estimate is insignificant. But, if a HR dataset is sparse, a rough prior estimate, based on a high density LR sample set, may contribute effectively for the fusion output, especially when predicting at the observation positions with sparse HR sample points.

Figure 13 presents a RA-based fusion example for a set of typical freeform surface measurement data from a tactile CMM and structured light (SL) scanner [63]. The CMM measurement is slow but highly accurate and 100 CMM sample points are used as the HR set. The SL measurement is fast but with large systematic error and 4695 SL sample points are used as the LR set. Reconstruction of each individual set with natural-neighbour interpolation produces large root-mean-square-error (RMSE), either due to the high measurement uncertainty of the SL set, or low sample density of the CMM set (see Figure 13b and c). Fusion of the two datasets with GP approximation or MBA successfully produces better reconstruction results with reduced errors.





(d) The error map of the RA-based fusion with GP approximation, RMSE = 0.22. (e) The error map of the RA-based fusion with MBA, RMSE = 0.17.

Figure 13. The performance of some residual approximation-based fusion methods (courtesy of [63]).

5. Summary and outlook

Holistic measurement of a workpiece is becoming the necessity in modern engineering. Workpieces with full 3D geometry or re-entrant features, or comprised of high-dynamic range structures, which need to be measured with multiple local measurements, are the driving force for the development of (multi-sensor) spatial data fusion techniques in surface and dimensional metrology. Some existing data fusion methods can be found in many non-tactile instruments based on image processing. However, fusion of spatial data is relatively new in surface metrology and only a small number of industrial applications have been implemented, in particular for the fusion of point cloud data.

Most spatial data fusion solutions under development follow a similar process framework comprised of pre-processes, registration, fusion and post-processes. The registration process has been widely investigated and some high quality algorithms are available. The fusion process is at an early stage and limited algorithms are in development. Among the existing fusion methods, residual approximation-based fusion solutions, in particular GP fusion, can be effective for both smooth and non-smooth surfaces, but the uncertainty propagation has not been analytically analysed. Weighted least-squares fusion based on linear systems can be efficient, but only applicable for surfaces with smooth geometry. The advantages and disadvantages, and versatility of these fusion solutions need to be further investigated.

Some post-processes have not been well resolved for spatial data fusion, such as data reduction, storage, rendering and other manipulations, with the assistance of a specialised spatial database management system. Therefore, the development of such spatial database management systems should form one of the next development phases for multi-sensor measurement techniques.

6. Acknowledgements

This work was funded by the UK National Measurement System Engineering & Flow Metrology Programme, the FP7 project NANOMend, European Research Council (ERC-ADG-228117) and the UK's Engineering and Physical Sciences Research Council (EP/I033424/1).

References

- [1] Weckenmann A, Jiang X, Sommer K D, Neuschaefer-Rube U, Seewig J, Shaw L and Estler T 2009 Multisensor data fusion in dimensional metrology *CIRP Ann.-Manuf. Techn.* **58**(2) 701-21
- [2] Jiang X and Whitehouse D J 2012 Technological shifts in surface metrology *CIRP Ann.-Manuf. Techn.* **61**(2) 815-36
- [3] Lonardo P M, Lucca D A, De Chiffre L 2002 Emerging trends in surface metrology *CIRP Ann.-Manuf. Techn.* **51**(2) 701-23
- [4] Bruzzone A A G, Costa H L, Lonardo P M and Lucca D A 2008 Advances in engineered surfaces for functional performance *CIRP Ann.-Manuf. Techn.* **57**(2) 750-69
- [5] De Chiffre L, Kunzmann H, Peggs G N and Lucca D A 2003 Surfaces in precision engineering, microengineering and nanotechnology *CIRP Ann.-Manuf. Techn.* **52**(2) 561-77

- [6] Hansen H N, Carneiro K, Haitjema H and De Chiffre L 2006 Dimensional micro and nano metrology *CIRP Ann.-Manuf. Techn.* **55**(2) 721-43
- [7] Evans C J and Bryan J B 1999 "Structured", "textured" or "engineered" surfaces *CIRP Ann.-Manuf. Techn.* **48**(2) 541-56
- [8] Segerman H 2012 3D printing for mathematical visualisation *Math. Intell.* **34**(4) 56-62
- [9] ISO 25178-6 2010 Geometrical product specifications (GPS) – surface texture: areal – part 6: classification of methods for measuring surface texture (Geneva: International Organization for Standards)
- [10] Carmignato S 2012 Accuracy of industrial computed tomography measurements: experimental results from an international comparison *CIRP Ann.-Manuf. Techn.* **61**(1) 491-4
- [11] Esteban J, Starr A, Willetts R, Hannah P and Bryanston-Cross P 2005 A review of data fusion models and architectures: towards engineering guidelines *Neural Comput. Appl.* **14**(4) 273-81
- [12] Leica Microsystems 2014 Leica DCM8 broucher <http://www.leica-microsystems.com>
- [13] GmbH W 2014 Automated confocal Raman and atomic force microscope alpha500 <http://www.witec.de/products/raman/alpha500/>
- [14] Kelly G 2000 Data fusion special interest group *Advanced Mathematical Tools in Metrology IV – Series on Advances in Mathematics for applied sciences* **53** (World Scientific Publishing)
- [15] JDL 1991 *Data fusion lexicon* (San Diego, USA)
- [16] Khaleghi B, Khamis A, Karray F O and Razavi S N 2013 Multisensor data fusion: a review of the state-of-the-art *Inform. Fusion* **14**(1) 28-44
- [17] Schabenberger O and Gotway C A 2014 *Statistical Methods for Spatial Data Analysis* (Taylor & Francis)
- [18] Dasarathy B V 1997 Sensor fusion potential exploitation-innovative architectures and illustrative applications *P. IEEE* **85**(1) 24-38
- [19] Ramasamy S K, Raja J and Boudreau B D 2013 Data fusion strategy for multiscale surface measurements *J. Micro Nano-Manuf.* **1**(1) 011004
- [20] Boudjemaa R, Forbes A B 2004 *Parameter estimation methods for data fusion* (National Physical Laboratory, UK)
- [21] Schervish M J 1987 A review of multivariate analysis *Stat. Sci.* **2**(4) 396-413
- [22] Otsubo M, Okada K and Tsujiuchi J 1994 Measurement of large plane surface shapes by connecting small-aperture interferograms *Opt. Eng.* **33**(2) 608-13
- [23] Kalman R E 1960 A new approach to linear filtering and prediction problems *J. Basic Eng.-T. ASME* **82**(1) 35-45
- [24] Leach R 2011 *Optical measurement of surface topography* (Springer)
- [25] ISO/DIS 25178-606 2013 Geometrical product specification (GPS) – surface texture: areal -- part 606: nominal characteristics of non-contact (focus variation) instruments (Geneva: International Organization for Standards)
- [26] Danzl R, Helml F and Scherer S 2011 Focus variation--a robust technology for high resolution optical 3D surface metrology *Stroj. Vestn.-J. Mech. E.* **57**(3).
- [27] ISO 25178-604 2013 Geometrical product specifications (GPS) – surface texture: areal – part 604: nominal characteristics of non-contact (coherence scanning interferometry) instruments (Geneva: International Organization for Standards)
- [28] Schmit J, Creath K and Wyant J C 2006 Surface profilers, multiple wavelength, and white light interferometry *Optical Shop Testing (3rd ed.)* (John Wiley & Sons) pp667-755
- [29] Caber P J 1993 Interferometric profiler for rough surfaces *Appl. Optics* **32**(19) 3438-41
- [30] Ai C and Novak E L 1997 Centroid approach for estimating modulation peak in broad-bandwidth interferometry (US Patent 5633715)
- [31] Bartsch M, Hilpert U, Goebbels J and Weidemann G 2007 Enhancement and proof of accuracy of industrial computed tomography (CT) measurements *CIRP Ann.-Manuf. Technol.* **56**(1) 495-8
- [32] Sun W, Brown SB and Leach RK 2012 *An overview of industrial X-ray computed tomography* (National Physical Laboratory, UK)
- [33] Feldkamp L A, Davis L C and Kress J W 1984 Practical cone-beam algorithm *J. Opt. Soc. Am. A.* **1**(6) 612-9
- [34] Tzung-Sz S, Jianbing H and Menq C H 2000 Multiple-sensor integration for rapid and high-precision coordinate metrology *IEEE/ASME T. Mech.* **5**(2) 110-121
- [35] Carbone V, Carocci M, Savio E, Sansoni G and De Chiffre L 2001 Combination of a vision system and a coordinate measuring machine for the reverse engineering of freeform surfaces *Int. J. Adv. Manuf. Tech.* **17**(4) 263-71
- [36] Motavalli S, Suharitdamrong V and Alrashdan A 1998 Design model generation for reverse engineering using multi-sensors *IIE Trans.* **30**(4) 357-66
- [37] Chen L-C and Lin G C I 1997 A vision-aided reverse engineering approach to reconstructing free-form surfaces *Robot. CIM-Int. Manuf.* **13**(4) 323-36
- [38] Machleidt T, Sparrer E, Dorozhovets N, Manske E, Franke K-H and Kapusi D 2009 Navigation in a large measurement volume by using AFM technology as a sensor system in the NPMM *Im-Tech. Mess.* **76**(5) 274-7
- [39] Manske E, Hausotte T, Mastlyo R, Hofmann N and Jäger G 2005 Nanopositioning and nanomeasuring machine for high accuracy measuring procedures of small features in large areas *Proc. SPIE* **5965** 09
- [40] Weisstein E W 2014 "Mean" <http://mathworld.wolfram.com/Mean.html>
- [41] Ramasamy S K 2011 *Multi-scale data fusion for surface metrology* (PhD Thesis, The University of North Carolina at Charlotte, US)
- [42] Otsubo M, Okada K and Tsujiuchi J 1992 Measurement of large plane surface shape with interferometric aperture synthesis *Proc. SPIE* **1720** 444
- [43] Catanzaro B E, Thomas J A and Cohen E J 2001 Comparison of full-aperture interferometry to subaperture stitched interferometry for a large-diameter fast mirror *Proc. SPIE* **4444** 224
- [44] Zhao C and Burge J H 2008 Stitching of off-axis sub-aperture null measurements of an aspheric surface *Proc. SPIE* **7063** 16
- [45] Jiang X, Wang K, Gao F and Muhamedsalih H 2010 Fast surface measurement using wavelength scanning interferometry with compensation of environmental noise *Appl. Optics* **49**(15) 2903-9
- [46] Ramasamy S K and Raja J 2013 Performance evaluation of multi-scale data fusion methods for surface metrology domain *J. Manuf. Syst.* **32**(4) 514-22
- [47] Raol J R 2009 *Multi-sensor data fusion with MATLAB®* (CRC Press)
- [48] Besl P J and McKay N D 1992 A method for registration of 3-D shapes *IEEE T. Pattern Anal.* **14**(2) 239-56
- [49] Hao C, Yan-ying L and Yan-jie W 2008 A novel image fusion method based on wavelet packet transform *IEEE International Symposium on Knowledge Acquisition and Modeling Workshop* (Wuhan, China) pp462-5
- [50] Yan-Mei C, Rong-Chun Z and Jin-Chang R 2004 Self-adaptive image fusion based on multi-resolution decomposition using wavelet packet analysis *Proceedings of 2004 International Conference on Machine Learning and Cybernetics* vol **7** pp4049-53
- [51] Yu S, Mantian L, Qingling L and Lining S 2006 A new wavelet based multi-focus image fusion scheme and its application on optical microscopy *IEEE International Conference on Robotics and Biomimetics* (Kunming, China) pp401-5
- [52] Santner T J, Williams B and Notz W 2003 *The Design and Analysis of Computer Experiments* (Springer)
- [53] Barker R M, Cox M G, Forbes A B and Harris P M 2004 *Best practice guide no. 4 software support for metrology: discrete modelling and experimental data analysis* (National Physical Laboratory, UK)

- [54] Zhang Z 1994 Iterative point matching for registration of free-form curves and surfaces *Int. J. Comput. Vision* **13**(2) 119-52
- [55] Low K-L 2004 Linear least-squares optimization for point-to-plane ICP surface registration (University of North Carolina at Chapel Hill, US)
- [56] Yamany S M and Farag A A 1999 Free-form surface registration using surface signatures *The Proceedings of the Seventh IEEE International Conference on Computer Vision* vol 2 pp1098-104 (Kerkyra, Greece)
- [57] Müller M, Krüger W and Saur G 2007 Robust image registration for fusion *Inform. Fusion* **8**(4) 347-53
- [58] Jiang X, Zhang X and Scott P J 2010 Template matching of freeform surfaces based on orthogonal distance fitting for precision metrology *Meas. Sci. Technol.* **21**(4) 045101
- [59] Qian Z, Seepersad C C, Joseph V R, Allen J K and Wu C F J 2005 Building surrogate models based on detailed and approximate simulations *J. Mech. Design* **128**(4) 668-77
- [60] Qian P Z G and Wu C F J 2008 Bayesian hierarchical modeling for integrating low-accuracy and high-accuracy experiments *Technometrics* **50**(2) 192-204
- [61] Kennedy M C and O'Hagan A 2000 Predicting the output from a complex computer code when fast approximations are available *Biometrika* **87**(1) 1-13
- [62] Xia H, Ding Y and Mallick B K 2011 Bayesian hierarchical model for combining misaligned two-resolution metrology data *IIE Trans.* **43**(4) 242-58
- [63] Colosimo B M, Pacella M and Senin N 2014 Multisensor data fusion via Gaussian process models for dimensional and geometric verification *Precis. Eng.* (In press)
- [64] Huang Y and Qian X 2006 A Dynamic Sensing-and-Modeling Approach to Three-Dimensional Point- and Area-Sensor Integration *J. Manuf. Sci. E.-T. ASME* **129**(3) 623-35
- [65] de Boor C 2001 *A practical guide to splines* (Springer)
- [66] Rasmussen C E and Williams C 2006 *Gaussian processes for machine learning* (the MIT Press)
- [67] Kjer H M and Wilm J 2010 Evaluation of surface registration algorithms for PET motion correction (Batchelor Thesis, Technical University of Denmark, Denmark)
- [68] Golub G H and Van Loan C F 1996 *Matrix Computations* (Johns Hopkins University Press)
- [69] Cazals F and Giesen J 2006 Delaunay triangulation based surface reconstruction *Effective Computational Geometry for Curves and Surfaces* ed J-D Boissonnat and M Teillaud (Springer) pp231-76
- [70] Raid I, Kusnezowa T and Seewig J 2013 Application of ordinary kriging for interpolation of micro-structured technical surfaces *Meas. Sci. Technol.* **24**(9) 095201
- [71] Krystek M 1996 Form filtering by splines *Measurement* **18**(1) 9-15
- [72] Levoy M 1988 Display of surfaces from volume data *IEEE Comput. Graph.* **8**(3) 29-37
- [73] Hansen C D and Johnson C R 2005 *The visualization handbook* (Burlington, MA: Butterworth-Heinemann)
- [74] Senin N, Blunt L A and Tolley M 2012 Dimensional metrology of micro parts by optical three-dimensional profilometry and areal surface topography analysis *P. I. Mech. Eng. B-J. Eng.* **226**(11) 1819-32
- [75] Garcia D 2010 Robust smoothing of gridded data in one and higher dimensions with missing values *Comput. Stat. Data An.* **54**(4) 1167-78
- [76] Hodge V J and Austin J 2004 A survey of outlier detection methodologies *Artif. Intell. Rev.* **22**(2) 85-126
- [77] Reinsch C H 1967 Smoothing by spline functions *Numer. Math.* **10**(3) 177-83
- [78] Rudin L I, Osher S and Fatemi E 1992 Nonlinear total variation based noise removal algorithms *Physica D* **60**(1-4) 259-68
- [79] Dobrev V, Guermond J and Popov B 2010 Surface reconstruction and image enhancement via l1-minimization *SIAM J. Sci. Comput.* **32**(3) 1591-616
- [80] Caselles V, Chambolle A and Novaga M 2007 The discontinuity set of solutions of the TV denoising problem and some extensions *Multiscale Model. Sim.* **6**(3) 879-94
- [81] Bustos B, Keim DA, Saupe D, Schreck T and Vrani DV 2005 Feature-based similarity search in 3D object databases *ACM Comput. Surv.* **37**(4) 345-87
- [82] Seeger S and Laboureyx X 2002 Feature extraction and registration: an overview *Principles of 3D Image Analysis and Synthesis, The Springer International Series in Engineering and Computer* (Springer Science & Business Media) vol **556** pp153-166
- [83] Bentley J L 1975 Multidimensional binary search trees used for associative searching *Commun. ACM.* **18**(9) 509-17
- [84] Faugeras O D and Hebert M 1986 The representation, recognition, and locating of 3-D objects *Int. J. Robot. Res.* **5**(3) 27-52
- [85] Masuda T, Sakaue K and Yokoya N 1996 Registration and integration of multiple range images for 3-D model construction *Proceedings of the 13th International Conference on Pattern Recognition* (Vienna, Austria) vol **1** pp879-83
- [86] Wang J 2012 *Sampling for the Measurement of Structured Surfaces* (PhD thesis, University of Huddersfield, UK)
- [87] Wang M Y, Fitzpatrick J M and Maurer C R 1995 Design of fiducials for accurate registration of CT and MR volume images *Proc. SPIE* **2434**
- [88] Inhull 2012 MATLAB File Exchange <http://www.mathworks.co.uk/matlabcentral/fileexchange/10226-inhull>.
- [89] Seungyong L, Wolberg G and Sung-Yong S 1997 Scattered data interpolation with multilevel B-splines *IEEE T. Vis. Comput. Gr.* **3**(3) 228-44
- [90] Diez DC 2005 *Adaptive Scattered Data Fitting with Tensor Product Spline-Wavelets* (PhD thesis, University of Bonn, Germany)
- [91] Strutz T 2010 *Data fitting and uncertainty: a practical introduction to weighted least squares and beyond* (Springer)
- [92] Abdul-Rahman H S, Jiang X and Scott P J 2013 Freeform surface filtering using the lifting wavelet transform *Precis. Eng.* **37**(1) 187-202
- [93] Fabio R 2003 From point cloud to surface: the modeling and visualization problem *International Archives of Photogrammetry, Remote Sensing and Spatial Information Sciences* **34**(5) W10
- [94] Shekhar S and Chawla S 2003 *Spatial Databases: A Tour* (Prentice Hall)
- [95] Piegl L A and Tiller W 1997 *The NURBS Book* (Springer)
- [96] Luo R C, Chih-Chen Y and Kuo-Lan S 2002 Multisensor fusion and integration: approaches, applications, and future research directions *IEEE Sens. J.* **2**(2) 107-19
- [97] Boyd S P and Vandenberghe L 2004 *Convex optimization* (Cambridge university press)
- [98] Mathworks 2014 *fmincon - find minimum of constrained nonlinear multivariable function* <http://www.mathworks.co.uk/help/optim/ug/fmincon.html>
- [99] Rasmussen C E and Nickisch H 2010 Gaussian processes for machine learning (GPML) toolbox *J. Mach. Learn. Res.* **11** 3011-5
- [100] Hemsley R 2009 *Interpolation on a magnetic field* (Bristol University, UK)